

Insights into the Reactions of Hydroxyl Radical with Diolefins from Atmospheric to Combustion Environments

Fethi Khaled, Binod Raj Giri, Dapeng Liu, Emmanuel Assaf, Christa Fittschen, and Aamir Farooq
J. Phys. Chem. A, **Just Accepted Manuscript** • DOI: 10.1021/acs.jpca.8b10997 • Publication Date (Web): 15 Feb 2019

Downloaded from <http://pubs.acs.org> on February 20, 2019

Just Accepted

“Just Accepted” manuscripts have been peer-reviewed and accepted for publication. They are posted online prior to technical editing, formatting for publication and author proofing. The American Chemical Society provides “Just Accepted” as a service to the research community to expedite the dissemination of scientific material as soon as possible after acceptance. “Just Accepted” manuscripts appear in full in PDF format accompanied by an HTML abstract. “Just Accepted” manuscripts have been fully peer reviewed, but should not be considered the official version of record. They are citable by the Digital Object Identifier (DOI®). “Just Accepted” is an optional service offered to authors. Therefore, the “Just Accepted” Web site may not include all articles that will be published in the journal. After a manuscript is technically edited and formatted, it will be removed from the “Just Accepted” Web site and published as an ASAP article. Note that technical editing may introduce minor changes to the manuscript text and/or graphics which could affect content, and all legal disclaimers and ethical guidelines that apply to the journal pertain. ACS cannot be held responsible for errors or consequences arising from the use of information contained in these “Just Accepted” manuscripts.

1
2
3
4 **Insights into the Reactions of Hydroxyl Radical with Diolefins**
5
6
7 **from Atmospheric to Combustion Environments**
8
9
10
11
12
13
14

15 Fethi Khaled¹, Binod Raj Giri^{1*}, Dapeng Liu¹, Emmanuel Assaf², Christa Fittschen², Aamir Farooq^{1*}
16
17
18
19

20 ¹King Abdullah University of Science and Technology, Clean Combustion Research Center, Physical
21
22 Sciences and Engineering Division, Thuwal 23955-6900, Saudi Arabia
23
24

25 ²Université Lille, CNRS, UMR 8522 – PC2A – Physicochimie des Processus de Combustion et de
26
27 l'Atmosphère, F-59000 Lille, France
28
29
30
31
32

33 *Corresponding Author: binod.giri@kaust.edu.sa
34 aamir.farooq@kaust.edu.sa
35
36
37
38
39
40
41
42
43
44
45
46
47
48
49
50
51
52
53
54
55
56
57
58
59
60

Abstract

Hydroxyl radicals and olefins are quite important from combustion and atmospheric chemistry standpoint. Large amounts of olefinic compounds are emitted into the earth's atmosphere from both biogenic and anthropogenic sources. Olefins make a significant share in the transportation fuels (e.g., up to 20% by volume in gasoline), and they appear as important intermediates during hydrocarbon oxidation. As olefins inhibit low-temperature heat release, they have caught some attention for their applicability in future advanced combustion engine technology. Despite their importance, the literature data for the reactions of olefins are quite scarce. In this work, we have measured the rate coefficients for the reaction of hydroxyl radicals (OH) with several diolefins, namely 1,3-butadiene, *cis*-1,3-pentadiene, *trans*-1,3-pentadiene, and 1,4-pentadiene, over a wide range of experimental conditions ($T = 294 - 468$ K and $p \sim 53$ mbar; $T = 881 - 1348$ K and $p \sim 1 - 2.5$ bar). We obtained the low- T data in a flow reactor using laser flash photolysis and laser induced fluorescence (LPFR/LIF), and the high- T data were obtained with a shock tube and UV laser-absorption (ST/LA). At low temperatures, we observed differences in the reactivity of *cis*- and *trans*-1,3-pentadiene, but these molecules exhibited similar reactivity at high temperatures. Similar to monoolefins + OH reactions, we observed negative temperature dependence for dienes + OH reactions at low temperatures – revealing that OH-addition channels prevail at low temperatures. Except for 1,4-pentadiene + OH reaction, which shows evidence of significant H-abstraction reactions even at low-temperatures, other diolefins studied here almost exclusively undergo addition reaction with OH radicals at the low-temperature end of our experiments; whereas the reactions mainly switch to hydrogen abstraction at high temperatures. These reactions show complex Arrhenius behaviour as a result of many possible chemical pathways in such a convoluted system.

1. Introduction

Global demands for petroleum-based liquid fuels is increasing at an average annual rate of ~1%¹ as the transport sector is almost entirely powered by internal combustion engines (ICEs) burning these fuels. The current scenario of renewable sources makes a slim outlook to surpass petroleum-based fuel in the foreseeable future, and the share of renewables will likely make up only ~ 10% even by 2040. Hence, ICEs will continue to power transport sectors to a large extent for decades to come. Curbing of environmental pollution and greenhouse gas emissions will thus remain a big challenge. At the present time, it seems that the best way to mitigate harmful impacts of transport system is to improve the combustion technology, e.g., by developing new fuel-engine systems. Lately, there has been a lot of interest on fuel-engine design optimization due to stringent emission restrictions and efficiency considerations worldwide.²⁻⁷ The aim of such studies is to optimize the fuel properties for the best performance in advanced low-temperature combustion modes.

Octane sensitivity (OS) of a fuel is an important metric for fuel-engine correlation which measures how differently a fuel responds to changing conditions such as intake temperature, intake pressure and compression ratio. OS is defined as the difference between research octane number (RON) and motor octane number (MON), i.e., $OS = RON - MON$. Kalghatgi^{2,4} proposed another metric, called the Octane Index (OI), to better characterize the antiknock property of a fuel. OI is given by $OI = RON - K \cdot OS$, where K is an empirical parameter determined experimentally in engines. As K is negative for most modern engines, a fuel with higher OS gives larger value of OI, and thereby it may allow an engine to operate more efficiently.^{2,4} Current trends in the development of more efficient spark ignition (SI) engines are towards increasing the compression ratios and implementing turbocharging.⁴ The challenge is that it may cause engine knocking as ignition delay times drop sharply with increasing cylinder pressure. As ignition delay times of high OS fuels tend to decrease less rapidly with increasing pressure, smaller chain olefinic fuels may provide the

1
2
3 desired antiknock quality. Unlike most paraffins, olefins have relatively high octane sensitivity
4 due to the presence of double bond(s), e.g., 1-butene (OS = 15.7), 2-ethyl-1-butene (OS = 18.9),
5 and 1-pentene (OS = 12.9) have much higher OS than *n*-butane (OS = 4) and *n*-heptane (OS = 0).⁸
6
7 These small chain olefinic fuels do not exhibit “cool flames” or negative temperature coefficient
8 (NTC) behavior due to the lack of low-temperature reactivity. Leppard⁹ and Westbrook et al.^{8, 10}
9
10 have discussed the connection between octane sensitivity of olefinic hydrocarbon fuels and the
11
12 lack of low-temperature reactivity. The inhibition of low-temperature reactivity of olefins is
13
14 attributed to the production of highly stable allylic type of radicals (resonance energy of ~14.3
15
16 kcal/mol for unconjugated and ≥ 19 kcal/mol for conjugated allyls)¹¹ following hydrogen
17
18 abstraction from the reactive allylic sites of olefins. In contrast to alkyl radicals, the allylic radicals
19
20 resist thermal decomposition or addition of molecular oxygen.
21
22
23
24
25
26
27
28
29

30
31 A significant amount of olefins, as high as 15 – 20%,¹⁰ is present in gasolines. They are also found
32
33 in other transportation fuels like aviation and diesel fuels. These olefins contribute substantially to
34
35 the octane rating and hence determine the ignition behavior of the fuel. Likewise, the degree of
36
37 unsaturation in biodiesels greatly affects their cetane quality, ignition delay times and CO/HC
38
39 emission.¹² Olefins also appear as important intermediates during hydrocarbon oxidation
40
41 processes. From combustion perspectives, dienes (C_nH_{2n-2}) are particularly interesting because of
42
43 the presence of two double bonds. The location of the double bonds (conjugated or not) and the
44
45 number and type of available allylic hydrogens alter the reactivity of olefinic molecules. For
46
47 example, 1,3-butadiene (C₄H₆) is the simplest conjugated diene which reacts with OH radicals by
48
49 roughly three times slower than that of 1-butene near 1200 K.¹³⁻¹⁵ 1,3-Butadiene builds up to a
50
51 significant concentration during combustion of hydrocarbon fuels.^{16,17} These works identified
52
53 C₄H₅, a resonantly stabilized radical, as being the major contributing factor for the formation of
54
55 the first aromatic ring. From combustion perspective, the resonantly stabilized radicals, their
56
57
58
59
60

1
2
3 addition reactions on the double bond(s), and cyclization processes are of great importance in the
4
5 understanding of the formation of the first aromatic ring and of the successive growth of polycyclic
6
7 aromatic hydrocarbons (PAH). Therefore, dienes contribute to the formation of benzene, a soot
8
9 precursor, and hence the chemistry of dienes govern the kinetics of soot formation processes.^{16, 17}
10
11 Kinetic studies about the oxidation behavior of dienes are quite scarce in the literature. Most of
12
13 the earlier studies were carried out near ambient temperatures.¹⁸⁻²⁵ At higher temperatures, only
14
15 1,3-butadiene caught the attention of most researchers.^{13, 26, 27} Li et al.²⁶ measured ignition delay
16
17 times of 1,3-butadiene in a shock tube and a rapid compression machine. Not surprisingly, they
18
19 observed a clear lack of NTC region due to the suppression of low-temperature reactivity of 1,3
20
21 butadiene. Li et al.²⁸ measured the rate coefficients for the reaction of 1,3-butadiene + OH at $T =$
22
23 240 – 340 K and $p \sim 1$ Torr in a discharge flow reactor using relative rate method. Their measured
24
25 rate coefficients exhibited negative temperature dependence given by the Arrhenius expression k
26
27 $(T) = (1.58 \pm 0.07) \times 10^{-11} \exp[(436 \pm 13)/T] \text{ cm}^3 \text{ molecule}^{-1} \text{ s}^{-1}$. In another work, Li et al.²⁷
28
29 performed a detailed theoretical analysis of H + 1,3-butadiene reaction over a wide range of
30
31 pressure and temperature. They found that H addition preferentially occurs (> 80%) at the terminal
32
33 carbon atom at all temperatures ($T = 298 - 2000$ K), whereas abstraction of H atom from the central
34
35 carbon atom is the dominant channel contributing more than 70% at all temperatures. Vasu et al.¹³
36
37 measured the rate coefficients of 1,3-butadiene + OH reaction over $T = 1011 - 1406$ K and $p \sim$
38
39 2.2 bar using shock tube and laser absorption technique. Additionally, they performed variational
40
41 transition-state theory using the parameters obtained from QCISD(T)/cc-pVT ∞ Z//B3LYP/6-
42
43 311++G(d,p) level of theory to rationalize terminal vs. non-terminal H atom abstraction. Their
44
45 total abstraction rate coefficients beyond 1200 K agreed very well with the experimentally
46
47 determined values. However, their theoretical values systematically underpredicted the measured
48
49 rate coefficients below 1200 K. They reasoned this to the opening of a new reaction channel at
50
51 lower temperatures, *i.e.*, addition of OH to the double bond of 1,3-butadiene. This indicates that
52
53
54
55
56
57
58
59
60

1
2
3 unlike monoalkenes + OH, addition of OH to dienes — depending upon the degree of conjugation
4 — can prevail at relatively higher temperatures. Therefore, dienes + OH are expected to show a
5
6 complex nature of temperature and pressure dependence of the rate coefficients due to the many
7
8 competing channels (addition, abstraction, back-dissociation, isomerization-and non-abstraction
9
10 bimolecular pathways). This warrants additional chemical kinetic studies beyond this simplest
11
12 conjugated diene (1,3-butadiene) to better characterize the reactions of dienes with OH radicals.
13
14
15
16
17
18

19 Olefins are not only important in combustion but also in atmospheric chemistry. Large amount of
20 these compounds is emitted into the earth's atmosphere from both biogenic and anthropogenic
21 sources, e.g., automobile emissions, evaporation of transportation fuels, forest fires, biogenic
22 isoprenes and terpenes.²⁹⁻³¹ OH initiated oxidation of olefins is one of the main pathways for the
23 fate of these hydrocarbons in the atmosphere.²⁵ The atmospheric chemistry of (poly)olefins are
24 more interesting as they offer more reaction pathways with OH radicals giving rise to larger rate
25 constants than that of (mono)olefins. Reactivity of a hydrocarbon with OH radicals in the
26 atmosphere also affects the formation of ozone. Peeters et al.²³ recently developed an approach
27 based on structure-activity relationship (SAR) to discern the site-specific addition of OH radicals
28 to the double bond(s) of olefins at 298 K. Their site-specific SAR approach provided excellent
29 predictive capabilities for the site-specific and total rate coefficients for 65 OH + (poly)olefin
30 reactions with an uncertainty of ~ 15%. From their detailed analysis, they showed that the total
31 rate coefficients of OH + (poly)olefins reactions may be accurately estimated by adding the
32 individual rate coefficients for the addition of OH radicals to the specific carbon-carbon double
33 bond(s) of (poly)olefin. Furthermore, they stated that this simple approach of summing up of site-
34 specific OH-addition rate coefficients is not valid for some compounds like α -terpinene and α -
35 phelandrene because significant contributions come from the abstraction of H atoms in such
36 molecules. For the reactions of α -terpinene and α -phelandrene with OH radicals, the deviations
37
38
39
40
41
42
43
44
45
46
47
48
49
50
51
52
53
54
55
56
57
58
59
60

1
2
3 in their SAR predicated values were as large as 40%. Ohta¹⁸ determined rate coefficients for 19
4 diolefin + OH reactions at ambient conditions utilizing relative rate method. Not surprisingly, they
5 observed an increase in the rate coefficients for diolefins + OH reaction with the increase of alkyl
6 substituents on the double bond(s). They showed that the reactivity of OH radicals with diolefins,
7 except allenes and cyclic diolefins, may be accurately estimated by summing up the rate coefficient
8 contributions from individual carbon-carbon double bonds. However, they had to multiply the rate
9 coefficients of analogous (mono)olefin by a factor of 1.24 to estimate the rate coefficients for
10 conjugated olefins + OH reactions. Ohta attributes this multiplication factor to the resonance effect
11 that promotes the addition of OH radicals to conjugated dienes. There are other SAR approaches^{18,}
12
13
14
15
16
17
18
19
20
21
22
23
24
25
26
27
28
29
30
31
32
33
34
35
36
37
38
39
40
41
42
43
44
45
46
47
48
49
50
51
52
53
54
55
56
57
58
59
60

21, 24, 25, 32-34 of varying degrees of accuracy in the literature.

From the discussion above, it is seen that OH + diolefins display very interesting chemistry, and that there are limited literature data available in quite narrow temperature and pressure ranges. Our current knowledge of these reactions is not adequate for the development of robust combustion and atmospheric models. Therefore, in the current work, we aim to provide new insights for OH + diolefins reactions by determining the rate coefficients of OH radicals with conjugated- π systems like 1,3-butadiene, *trans*- and *cis*-1,3-pentadiene, and non-conjugated- π systems like 1,4-pentadiene. The trends observed will be discussed and analyzed to rationalize the reactivity of diolefins with OH radicals.

2. Experimental Method

We investigated the reactions of OH radicals with 1,3-butadiene (1,3-C₄H₆, R1), stereo-isomers of 1,3-pentadiene (*cis*-1,3-C₅H₈, R2; *trans*-1,3-C₅H₈, R3) and 1,4-pentadiene (1,4-C₅H₈, R4) over a wide range of experimental conditions using a low-pressure shock tube facility ($T = 881 - 1348$

1
2
3 K, $p \sim 1 - 2.5$ bar) at King Abdullah University of Science and Technology (KAUST) and a laser
4
5 photolysis flow reactor ($T = 294 - 468$ K, $p \sim 53$ mbar) at University of Lille.
6
7



21 **Shock Tube/Laser Absorption (ST/LA):** As the details of the ST/LA technique are provided
22
23 in our earlier works^{35,36}, here, we describe the experimental setup very briefly. The stainless steel
24
25 shock tube has an inner diameter of 14.2 cm, and consists of a 9 m long driven section and a
26
27 variable length driver section. For this work, we used a 3 m long driver section to achieve an
28
29 adequate reaction time of ~ 1.5 ms behind reflected shock waves. We used a polycarbonate
30
31 diaphragm of thickness 5 mm to separate the driven section from the driver section and to achieve
32
33 reflected shock pressure of ~ 1.5 atm. We generated shock waves by pressure bursting of the
34
35 diaphragm. The shock wave propagated into the driven section, heating and pressurizing the test
36
37 gas mixture almost instantaneously. We employed a series of five PCB 113B26 piezoelectric
38
39 pressure transducers, placed in the last 1.3 m of the driven section, to measure the incident shock
40
41 speed. We used the shock speed and initial temperature / pressure of the shock tube to calculate
42
43 the temperature and pressure behind the reflected shock wave. For these calculations, we used the
44
45 Frosh code³⁷ which is based on shock-jump relations³⁸.
46
47
48
49
50
51
52

53 We used a narrow-width Spectra-physics dye laser system to generate ultra-violet (UV) light
54
55 near ~ 307 nm. We achieved a UV light beam of 307 nm by the external frequency doubling of
56
57 red light (614 nm), produced by a ring-dye cw laser, which is pumped at 532 nm by a solid state
58
59
60

1
2
3 Nd:YAG laser. We tuned the UV light precisely to the center (306.6868 nm) of the well-
4 characterized R1(5) line in the (0, 0) absorption band of the $A^2 \Sigma^+ \leftarrow X^2 \Pi$ electronic transition of
5 OH radical. We used two quartz optical windows at 2 cm away from the endwall to guide UV light
6
7
8
9
10 beam into the reaction zone of the shock tube for OH detection. We chose *tert*-butyl hydroperoxide
11 (TBHP) for OH radical source as it decomposes very rapidly (half-life $\leq 5 \mu\text{s}$ for $T > 800 \text{ K}$) to
12 generate OH and $(\text{CH}_3)_3\text{CO}$ radicals.³⁹ We employed two modified Thorlab PDA36-EC
13 photodetectors to measure the laser intensity before and after the shock tube. The noise of the laser
14 beam after common-mode-rejection was lower than 0.1% of the signal. Using Beer-Lambert law,
15 absorbance (A) = $\ln(I_0/I) = X_{\text{OH}}k_{\text{OH}}PL$, we quantitatively converted laser-intensity time profile into
16 OH mole fraction (X_{OH}) time profile. Here, I and I_0 are the transmitted and incident laser intensities,
17 k_{OH} stands for the OH-absorption coefficient at 306.68 nm, P and L are the total pressure and the
18 optical path-length (14.2 cm), respectively.
19
20
21
22
23
24
25
26
27
28
29
30
31
32
33

34 **Laser Photolysis Flow Reactor/Laser Induced Fluorescence (LPFR/LIF):** Low-temperature
35 experiments for the reactions of OH radicals with dienes were carried out using LPFR/LIF
36 technique; the details of which can be found elsewhere.^{40,41, 42} Here, only a brief description is
37 given. The flow reactor is a stainless steel cell that is equipped with external heating coil.
38 Temperatures up to 500 K are attainable inside the reactor, and the temperature at the center of the
39 reactor is read using a fast response thermocouple within an uncertainty of 1 K. The photolysis
40 beam enters the long axis of the flow reactor *via* a quartz window and generates OH radicals after
41 laser flash photolysis of H_2O_2 at 248 nm. The photolysis laser beam was produced by an excimer
42 laser (Lambda Physik LPX 201) operating at a repetition rate of 1 Hz and a laser fluence of ~ 70
43 mJ cm^{-2} . This repetition rate ensured an adequate time for the complete replenishment of the
44 gaseous mixtures inside the flow reactor between successive laser photolysis pulses. Furthermore,
45 photolysis beam intensity was checked at both the entrance and the exit of the flow reactor to
46
47
48
49
50
51
52
53
54
55
56
57
58
59
60

1
2
3 ensure spatial (axial) uniformity of OH radical concentration.⁴² For OH excitation, the probe laser
4 beam was introduced through the short axis of the reactor, perpendicular to the photolysis beam.
5
6 The probe laser light at 282 nm was produced by frequency doubling of a dye laser (Sirah Laser
7 PrecisionScan PRSC-24-HPR, rhodamine 6G dye). This dye laser was pumped by the frequency-
8 doubled output of an Nd:YVO₄ laser (Spectra Physics Navigator II YHP40-532QW). The probe
9 laser has an output beam power of ~35 mW and a repetition rate of 10 kHz. The synchronisation
10 between the photolysis and probe beam was controlled with the help of a delay generator
11 (Princeton Research 9650).
12
13
14
15
16
17
18
19
20
21
22
23

24 Hydroxyl radical excitation at 282 nm corresponds to the (1,0) vibrational band of the A-X
25 electronic transition. Following OH radical excitations at 282 nm, OH radical decay was monitored
26 by capturing the laser induced fluorescence (LIF) signals leaking out of the axis perpendicular to
27 both the photolysis and probe beam. The red-shifted fluorescence signals were detected at ~308
28 nm by a photomultiplier (Hamamatsu R212) after passing through an interference filter (308 ± 10
29 nm). As the excitation laser was operated at 10 kHz giving data point every 100 μs, the LIF signal
30 was acquired for 1 s corresponding to 10,000 data points, i.e., 5000 data points were recorded
31 before each photolysis pulse to measure the background signal and 5000 data points after the
32 photolysis pulse. Each data point was summed over ~100 photolysis pulses. The details of
33 synchronization of various units and data acquisition can be found elsewhere.^{40,41, 42}
34
35
36
37
38
39
40
41
42
43
44
45
46
47
48
49

50 **Chemicals and Mixture Composition:** We purchased 1,3-butadiene (99% purity), 1,4-
51 pentadiene (99%), and *tert*-butyl-hydroperoxide aqueous solution (TBHP, 30% solution in water)
52 from Sigma Aldrich, whereas *cis*-1,3-pentadiene (89% purity) and *trans*-1,3-pentadiene (95%
53 purity) were purchased from ChemSampCo. As per vendors data sheet, the main impurities of *cis*-
54 1,3-pentadiene are *trans*-1,3-pentadiene (1.79%), 2-methyl-2-butene (0.44%), cyclopentene
55
56
57
58
59
60

(0.61%) and cyclopentane (8.36%). *Trans*-1,3-pentadiene contained cyclopentane (3.2%) and *cis*-1,3-pentadiene (1.8%) as impurities. We obtained argon and helium from AH Gases, and their purity was 99.999%. For ST/LA experiments, we prepared gas mixtures, diluted in argon, manometrically in a 24-litre teflon-coated stainless-steel vessel equipped with a magnetically-driven stirrer. The mixtures were left to homogenize for at least one hour. As for LPFR/LIF experiments, dilute mixtures of dienes in helium were prepared in a glass bulb. Prior to preparation of gas mixtures, the mixing vessel or glass bulb was turbo-pumped down to $<10^{-5}$ Torr. Table 1 compiles the mixture compositions used in this work.

Table 1: Mixture composition for ST/LA and LPFR/LIF experiments with argon and helium as diluents, respectively.

Reaction system	ST/LA experiments		LPFR/LIF experiments	
	[Fuel]	[TBHP]	[Fuel]	[H ₂ O ₂]
1,3-butadiene	356-514 ppm*	~18 ppm*	15-70 ppm	0.3-3 ppm
<i>cis</i> -1,3-pentadiene	300-400 ppm	10-20 ppm	3-30 ppm	0.3-3 ppm
<i>trans</i> -1,3-pentadiene	300-500 ppm	10-20 ppm	3-30 ppm	0.3-3 ppm
1,4-pentadiene	250-400 ppm	10-20 ppm	3-30 ppm	0.3-3 ppm

*: Data are taken from the work of Vasu et al.¹³

As seen in Table 1, we carried out all experiments with excess concentration of dienes as compared to OH radicals. Under such conditions, one may expect the measured OH decay to follow the first-order kinetics, and the decay of OH radicals will mainly be governed by the reaction under investigation. For ST/LA experiments, we used a ratio for fuel to TBHP of 20 or higher, and for LPFR/LIF experiments, we introduced the dilute mixtures of dienes into the flow reactor by adding a small flow of the mixture to the main flow of helium through calibrated mass flow controllers.

1
2
3 We obtained a variable concentration of water-free H₂O₂ in the flow reactor by adjusting the flow
4 of helium through the flask containing a mixture of urea-H₂O₂ powder and SiO₂ at 40 °C. We
5 obtained a typical concentration of H₂O₂ $\sim 1 \times 10^{14}$ cm⁻³ *via* the thermal decomposition of H₂O₂-
6 urea mixture. By adjusting the flow, we were able to determine an optimum working condition
7 that gave us a sufficiently low background signal and a good signal-to-noise ratio for OH traces.
8
9
10
11
12
13
14

15 3. Results and discussion

16
17 **High-Temperature Kinetics.** High-temperature data were obtained behind reflected shock waves
18 using ST/LA technique for a wide range of experimental conditions ($T = 881 - 1348$ K, $p \sim 1 -$
19 2.5 bar). Figure 1 displays a representative OH time-history measured at $T = 1116$ K and $p = 1.41$
20 bar for a case of 300 ppm *cis*-1,3-pentadiene, 20 ppm TBHP diluted in argon. The inset in Fig. 1
21 illustrates an example of pseudo-first order decay of OH radicals, justifying well-tailored mixture
22 compositions. However, the overall reaction rate coefficients were obtained from detailed kinetic
23 modeling to account for the contributions from secondary chemistries. Our kinetic model is
24 composed up of sub-mechanism for TBHP chemistry taken from Pang et al.⁴³ with updates for
25 the sensitive reactions from Badra et al.³⁵ and Mehl et al.⁴⁴ gasoline surrogate mechanism that
26 contains the sub-mechanism for 1,3-pentadiene and 1,4-pentadiene. The best fit to the
27 experimentally measured profiles was obtained by treating the rate coefficient of the target reaction
28 as variable. The red line in Fig. 1 shows an example of such a best fit, and also shown is the effect
29 of $\pm 30\%$ perturbations from the best value ($k_2 = 2.45 \times 10^{-11}$ cm³ molecule⁻¹ s⁻¹ at 1116 K, 1.41 bar
30 for R2). Table 2 compiles the current measurements for the overall high-temperature rate
31 coefficients of *cis*-1,3-Pentadiene + OH (R2) and *trans*-1,3-Pentadiene + OH (R3) reactions.
32
33
34
35
36
37
38
39
40
41
42
43
44
45
46
47
48
49
50
51
52
53
54
55
56
57
58
59
60

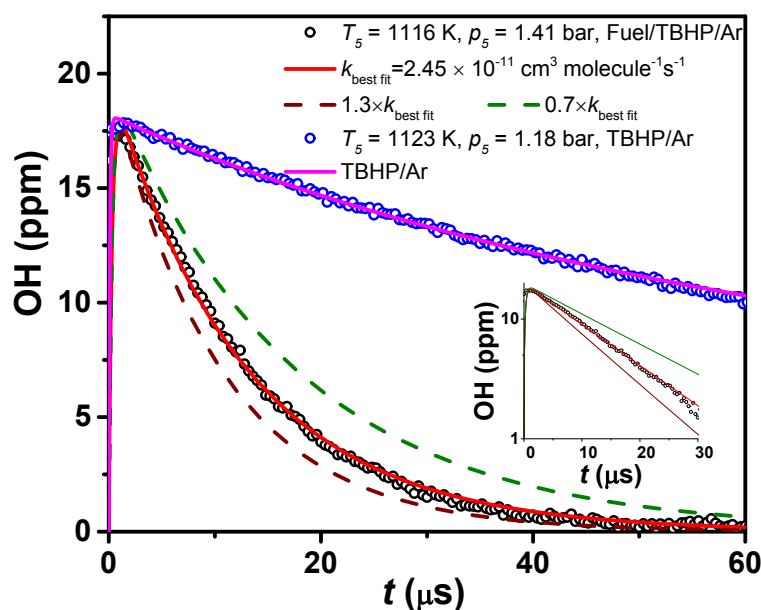


Figure 1: A typical OH time profile measured during OH + *cis*-1,3-pentadiene reaction (R2) using ST/LA technique. Mixture composition: 300 ppm *cis*-1,3-pentadiene, 20 ppm TBHP in argon. The best fit indicated by red line corresponds to a rate coefficients of $2.45 \times 10^{-11} \text{ cm}^3 \text{ molecule}^{-1} \text{ s}^{-1}$, dashed lines show a $\pm 30\%$ perturbation from the best value. Inset figure shows $\ln[\text{OH}]$ vs time plot to demonstrate that OH decay obeys pseudo-first order kinetics. Blue symbols represent a control experiment for OH time history carried out for a mixture of TBHP in argon without fuel.

Table 2: Overall high-temperature rate coefficients for *cis*-1,3-pentadiene + OH (R2) and *trans*-1,3-pentadiene + OH (R3) reactions. The uncertainties in the rate coefficient are $+11\% / -9\%$ (see Table 3).

<i>cis</i> -1,3-pentadiene + OH (R2)			<i>trans</i> -1,3-pentadiene + OH (R3)		
T (K)	p (bar)	k_2 ($10^{-11} \text{ cm}^3 \text{ molecule}^{-1} \text{ s}^{-1}$)	T (K)	p (bar)	k_3 ($10^{-11} \text{ cm}^3 \text{ molecule}^{-1} \text{ s}^{-1}$)
909	1.55	1.78	881	1.36	1.50
918	1.75	1.66	921	1.58	1.80
951	1.33	1.84	936	1.81	1.69
972	1.68	1.73	1006	1.76	1.92
989	1.33	1.89	1025	1.22	1.96
989	1.25	2.03	1034	1.24	2.11
1004	1.15	1.92	1047	1.7	2.14
1024	1.32	2.02	1056	1.28	1.87
1028	1.65	1.82	1059	1.18	2.02
1067	1.59	2.04	1073	1.21	2.05
1110	1.54	2.13	1121	1.78	2.15
1116	1.41	2.45	1139	1.22	2.19
1136	1.2	2.34	1144	1.72	2.20
1166	1.52	2.26	1147	1.23	2.37

1168	1.3	2.42	1159	1.15	2.40
1216	1.36	2.56	1202	1.6	2.18
1236	1.54	2.44	1215	1.17	2.38
1236	1.53	2.44	1245	1.56	2.47
1252	1.14	2.66	1273	1.38	2.64
1282	1.51	2.57	1273	1.46	2.55
1330	1.53	2.92			

We determined uncertainty bounds in our measured rate coefficients by identifying and quantifying various sources of errors. The error sources and the estimated uncertainties in the measured rate coefficients of the targeted reaction are listed in Table 3. While determining the magnitude of each individual error source, the error source was perturbed to the lower and upper bounds to acquire the best fit to the experimentally measured OH profiles by adjusting the rate coefficient of the target reaction. By doing so, the uncertainties in the rate coefficients from all error sources were quantified at a particular temperature and pressure and later lumped together using the root-mean-square method. We did not incorporate mole fractions of impurity components in our kinetic model to determine their uncertainty contributions to the measured rate coefficients. Instead, we simply estimated the total rate coefficients for OH reactions with the individual impurity components and added these together to get a final value of the rate coefficient that translated into a percentage error in the overall measured rate coefficients. Our estimate suggests that all impurity components present in *cis*-1,3 pentadiene induce 1% and 8% errors in the measured overall rate coefficients at 1000 K and 298 K, respectively; whereas the induced errors for *trans*-1,3 pentadiene is even less, 0.5% and 4%, respectively. The overall uncertainty of the measured rate coefficients for R2 and R3 was found to be +11% / -9% at 1000 K and 1.5 bar.

Table 3: Uncertainty quantification of high-temperature rate coefficients for OH reactions with *cis*-1,3-pentadiene (R2) and *trans*-1,3-pentadiene (R3)

Uncertainty source	Uncertainty bounds		Uncertainty in k_2 and k_3	
	<i>cis</i> -1,3-pentadiene	<i>trans</i> -1,3-pentadiene	<i>cis</i> -1,3-pentadiene	<i>trans</i> -1,3-pentadiene
Temperature	±2%			2%
Impurity(%)	±11%	±5%	1%	0.5%
Fuel concentration (%)		±5%		5%
Fitting procedure		5%		5%
OH absorption signal noise		3%		1%
Secondary chemistry	TBHP + OH ⇒ TBUTOXY + OH, ±30%		5% for T <1000K, 0.5% for T >1000K	
	CH ₃ + OH ⇒ CH ₂ + H ₂ O, factor of 2			3%
Others (absorption coefficients, pressure ...)				3%
Root-mean-square error			+11% / -9%	+11% / -9%

Figure 2 displays Arrhenius plots for the overall rate coefficients of reactions R1 – R4 measured in this work along with literature data of straight chain olefins for comparison. As can be seen, these olefins display very interesting reactivity towards OH radicals by exhibiting severe curvature of varying degree for the temperature dependence of the rate coefficients. Such complex Arrhenius behavior, shown by these olefins + OH reactions, is the result of the combined effect stemming from various chemical processes, e.g., abstraction, addition, back dissociation and non-abstraction

bimolecular channels. Of course, the complexity of (poly)olefins + OH reactions depend upon their underlying potential energy surfaces, and the accuracy of the potential energy surfaces will determine the quality of the predicted rate coefficients for these individual chemical processes. As we will discuss low-temperature chemistry in the next section, we focus here on the high-temperature reactivity trends of these olefins (conjugated or unconjugated) with OH radicals to draw some useful conclusions. As stated earlier, there are limited high-temperature literature data for diolefins + OH reactions for meaningful comparison.

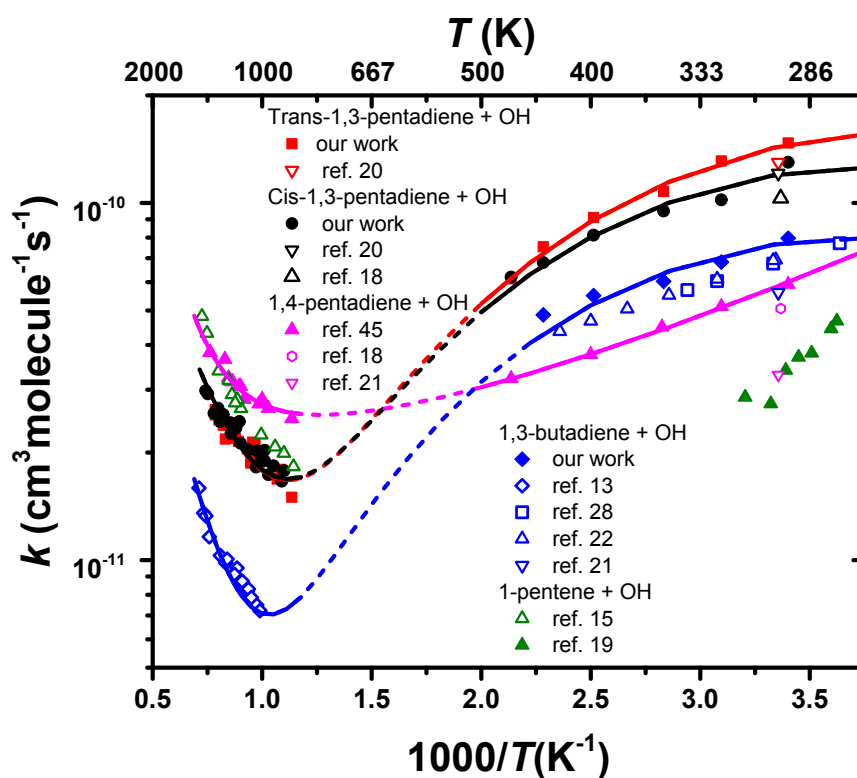


Figure 2: Arrhenius plot for the total rate coefficients of OH radical reactions with 1,3-butadiene (R1), *cis/trans*-1,3-pentadiene (R2 and R3) and 1,4-pentadiene (R4) along with selected literature data: 1,3-butadiene [13, 21, 22, 28]; *trans* and *cis*-1,3-pentadiene from Magneron et al.²⁰; *cis*-1,3-pentadiene from Ohta et al.¹⁸; 1,4-pentadiene high temperature data from Giri et al.⁴⁵; 1-pentene from Khaled et al.¹⁵ and McGillen et al.¹⁹. Lines represent the best fit to the experimental rate coefficients that can be best described by eqs. 1 – 4. Due to the complex nature of these (poly)olefins + OH reactions, the broken lines caution the users for using eqs. 1 – 4 to obtain total rate coefficients in the intermediate temperature region.

First, we notice that both *cis*- and *trans*-1,3 pentadiene exhibit similar reactivity under high-temperature conditions (see Fig. 2). This may indicate that these isomers have isomerized quickly

1
2
3 to yield equilibrated population of both conformers before undergoing reaction with OH radicals.
4
5 Our finding appears to resonate well with the results of Marley et al.⁴⁶ who studied the
6
7 isomerization reaction of *cis*- and *trans*-1,3-pentadiene in the shock tube and reported an
8
9 isomerization rate expression of $k_{cis \rightarrow trans} = 10^{13.6} \exp(-63000/4.58T) \text{ s}^{-1}$ resulting in $t_{1/2} \leq 0.5 \mu\text{s}$ for
10
11 $T \geq 800 \text{ K}$. However, we are not certain about this rate expression as the authors are not consistent
12
13 with their reported values of the Arrhenius parameters. For example, they used $A_\infty = 13.6 \text{ s}^{-1}$ and
14
15 $E_a = 53 \text{ kcal/mole}$ in another occasion and stated that the conversion was very small and that they
16
17 never reached equilibrium in their experiments for the residence time of $150 \mu\text{s}$. That being said,
18
19 *cis*- and *trans*-1,3-pentadiene may not undergo fast isomerization even at high temperatures, and
20
21 that they would still retain their conformational identity. If it is so, then one would expect *trans*-
22
23 1,3-pentadiene to react somewhat faster than *cis*-1,3-pentadiene, similar to that observed in the
24
25 reactions of *cis/trans*-2-pentene and *cis/trans*-2-hexene with OH radicals at high temperatures.¹⁵
26
27 But, we do not observe any differences in the reactivity for the plausible reason being that the
28
29 expected reactivity differences are masked within the reported uncertainty of $\pm 10\%$ of our
30
31 experiments.
32
33
34
35
36
37

38
39 Secondly, we observed that these diolefins + OH reactions exhibit pronounced positive
40
41 temperature dependence at high temperatures, revealing that these reactions primarily undergo
42
43 chemical pathways having sizable energy barriers, e.g., hydrogen abstraction and/or non-
44
45 abstraction bimolecular pathways. The reactions of OH radicals with *cis*- and *trans*-1,3
46
47 pentadienes display a weaker T -dependence and larger rate coefficients by a factor of ~ 3 as
48
49 compared to 1,3-butadiene. Note that both are conjugated diolefins, and that the barrier heights
50
51 and relative energies of the product radicals, following OH addition to the terminal carbon atom
52
53 of C=C, are expected to be comparable due to similar resonance energy of the stabilized adduct
54
55 radicals. This means the contribution of the addition channels in both cases might be of comparable
56
57 magnitude, and consequently, as the C-H vinylic bond is strong (bond dissociation energy ≥ 108
58
59
60

1
2
3 kcal/mole)⁴⁷ and their removal *via* abstraction is slow, the difference in the reactivity and
4
5 temperature dependence comes largely from the abstraction of comparatively loosely bound –CH₃
6
7 allylic hydrogens atoms (BDE = 82 – 85 kcal/mole)⁴⁷ in *cis-/trans*-pentadienes which are absent
8
9 in 1,3-butadiene. At high temperatures, if we were to estimate the overall rate coefficients by
10
11 summing up all the site-specific rate coefficients for hydrogen abstractions^{13, 48} of 1,3-pentadiene,
12
13 i.e., $k_{\text{overall}}(T) = k_{\text{abstraction}}(T) + k_{\text{addition}}(T) + k_{\text{non-abstraction}}(T) \approx k_{\text{abstraction}}(T) \approx 2 \times k_{\text{terminal (vinylic)}}(T) +$
14
15 $3 \times k_{\text{non-terminal (vinylic)}}(T) + 3 \times k_{\text{allyl}}(T)$, we obtain a very good match between our experimental data
16
17 and predicted rate coefficients at the high-temperature end of our experiments, e.g., $k_{\text{overall}}(T =$
18
19 1330 K) for the experimentally measured and estimated values are $2.92 \times 10^{-11} \text{ cm}^3 \text{ s}^{-1}$ and $2.85 \times$
20
21 $10^{-11} \text{ cm}^3 \text{ s}^{-1}$, respectively. However, the deviations are large at lower temperatures (as large as
22
23 30% near 1000 K), where the predicted rate coefficients systematically underpredict our
24
25 experimental data. Similar observations were made by Vasu et al.¹³ for 1,3-butadiene + OH
26
27 reaction. At temperatures lower than 1200 K, their measured rate coefficients were larger (~20%
28
29 at 1000K) than their theoretical predictions. This may allow us to conclude that, for conjugated
30
31 diolefins + OH reactions, addition and/or non-abstraction bimolecular channels contribute
32
33 significantly to the overall rate coefficients even at temperatures as high as 1000 K. The reason
34
35 being that, unlike (mono)olefin + OH reactions, addition of OH radicals to these conjugated
36
37 diolefins preferentially yield resonantly stabilized adduct radicals that land into a deeper well (see
38
39 reference¹³ and references cited therein). The resulting stabilized radicals can now live longer,
40
41 thereby opening up new channels at lower temperatures. These resonantly stabilized adduct
42
43 radicals react slowly with molecular oxygen which suppresses the low-temperature combustion
44
45 behaviour of these conjugated diolefins. Nonetheless, hydrogen abstraction reactions prevail for
46
47 these dienes + OH reactions at high temperatures, and their role becomes increasingly important
48
49 if sp² carbon atoms are replaced with sp³ and/or conjugation is broken by inserting sp³ hybridized
50
51 carbon atoms in the (poly)olefin molecular skeleton. This is seen when one compares the overall
52
53
54
55
56
57
58
59
60

1
2
3 rate coefficients for OH radical reactions with 1-pentene and 1,3-pentadiene. As seen in Fig. 2, 1-
4
5 pentene reacts faster than 1,3-pentadiene, indicating that H-abstraction pathways are the main
6
7 active routes at high temperatures. Among the olefins studied here, 1,4-pentadiene displays the
8
9 highest reactivity towards OH radicals. This is probably not surprising because of the ease of
10
11 hydrogen abstraction from the bis-allylic position. Due to super-resonance stabilization of the
12
13 incipient radical, the abstraction pathway from the bis-allylic site is expected to be more kinetically
14
15 and thermodynamically favorable as compared to the other abstraction pathways available for
16
17 these olefins. The weak positive-temperature dependence and high reactivity of 1,4-pentadiene
18
19 with OH radicals points to small but sizable barrier height(s) for the abstraction and/or non-
20
21 abstraction bimolecular pathway(s).
22
23
24
25
26
27

28 **Low-Temperature Kinetics.** We obtained low-temperature data for reactions R1-R4 in a flow
29
30 reactor using laser flash photolysis and laser induced fluorescence (LPFR/LIF) technique over the
31
32 temperature range of 291 to 468 K and pressure ~ 53 mbar. Figure 3 shows a typical LIF signal of
33
34 OH radicals, as detected by the photomultiplier for a mixture of H_2O_2 and 2.81×10^{13} molecule
35
36 cm^{-3} *cis*-1,3-pentadiene in helium; also shown is the OH-LIF signal for a control experiment
37
38 carried out for a mixture of H_2O_2 and He only.
39
40
41
42
43
44
45
46
47
48
49
50
51
52
53
54
55
56
57
58
59
60

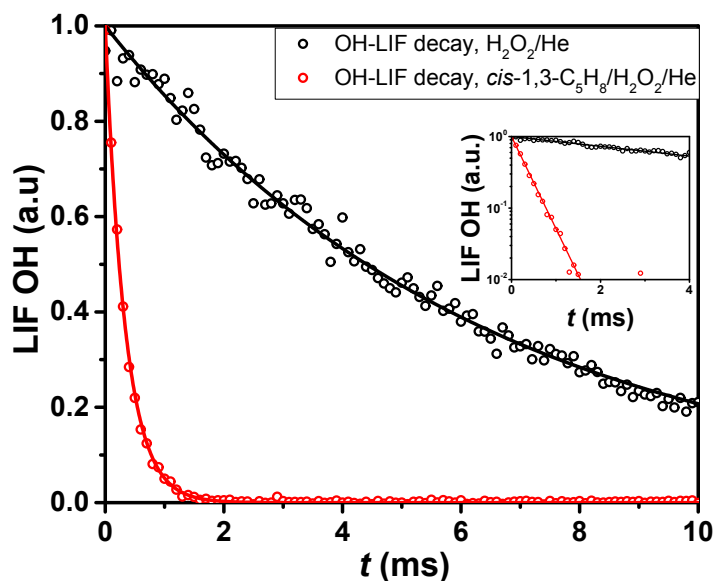


Figure 3: Red symbols show a typical OH-LIF decay time profile measured during OH + *cis*-1,3-pentadiene reaction (R2) at 323 K and 48 mbar using LPFR/LIF technique; black symbols represent OH-LIF decay time profile recorded in a control experiment.

As can be seen in Fig. 3, OH-LIF signal decays following first-order kinetics, i.e., $\ln[\text{OH}]$ vs time plot yields a straight line with a slope $(k_{\text{pseudo}}) = k_{\text{bi}} [\text{Fuel}]$. The bimolecular rate constant (k_{bi}) can be readily obtained by dividing the slope with the fuel concentration. Alternatively, the bimolecular rate coefficient (k_{bi}) may also be obtained from the slope of OH-LIF signal as a function of fuel concentration as illustrated in Fig. 4 for *cis*-1,3-pentadiene + OH reaction. The slope of each straight line represents the rate coefficient of the target reaction at the corresponding temperature. The intercept of this plot represents the OH decay arising mostly from the reaction of OH radicals with the precursor H_2O_2 as well as diffusion out of the observation volume. Secondary chemistry, such as $\text{OH} + \text{OH} = \text{H}_2\text{O}_2$ play a minor role.

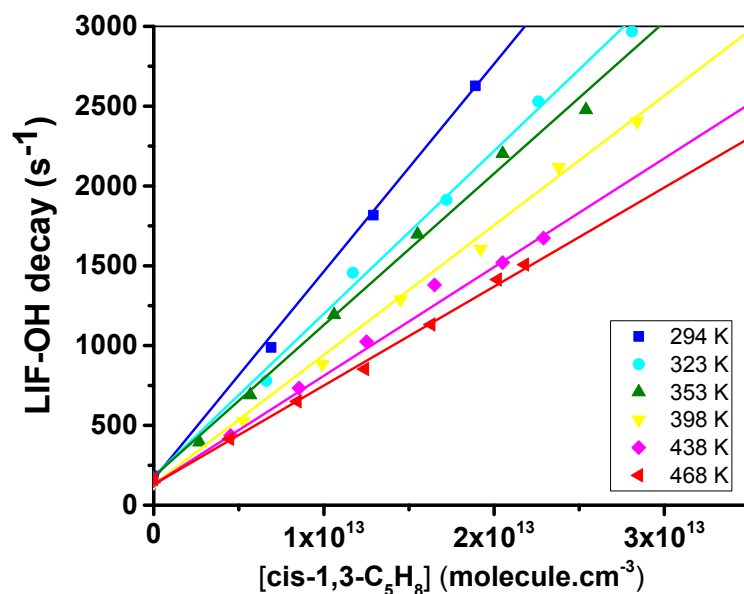


Figure 4: A typical plot for OH-LIF decay constant as a function of cis-1,3-pentadiene concentration. The slope of each line corresponds to the overall rate coefficient of OH + cis-1,3-pentadiene at the given temperature.

In a similar manner, the rate coefficients for OH reactions with other diolefins, 1,3-butadiene, *trans*-1,3-pentadiene and 1,4-pentadienes, were obtained. Table 4 compiles the measured overall rate coefficients at low temperatures. Figure 2 compares measured rate coefficients with the available literature data for 1,3-butadiene, *cis/trans*-pentadiene, and 1,4-pentadiene. As explained earlier for high-temperature measurements, we adopted similar methodology to quantify uncertainties for the measured data at low temperatures. Table 5 summarizes the error sources and resulting uncertainties in our measured overall rate coefficients which were found to be 7%, 11%, 8% and 7% for R1, R2, R3 and R4, respectively.

Table 4: Overall low-temperature rate coefficients ($p \sim 53$ mbar) for OH reactions with 1,3-butadiene (R1), *cis*-1,3-pentadiene (R2), *trans*-1,3-pentadiene (R3) and 1,4-pentadiene (R4). See Table 5 for uncertainty in the measured rate coefficients.

$T(\text{K})$	$k_1 - k_4$ (10)			
	1,3-butadiene	<i>cis</i> -1,3-pentadiene	<i>trans</i> -1,3-pentadiene	1,4-pentadiene
294 K	7.96	13.0	14.7	5.92
323 K	6.83	10.2	13.1	5.13
353 K	6.03	9.49	10.8	4.492
398 K	5.51	8.12	9.11	3.77
438 K	4.86	6.81	7.53	--
468 K	--	6.20	6.13	3.22

Table 5: Uncertainty quantification of low-temperature rate coefficients for OH reactions with 1,3-butadiene (R1), *cis*-1,3-pentadiene (R2), *trans*-1,3-pentadiene (R3) and 1,4-pentadiene (R4).

Uncertainty source	Uncertainty bounds				Uncertainty to k_1-k_4			
	1,3-butadiene	<i>cis</i> -1,3-pentadiene	<i>trans</i> -1,3-pentadiene	1,4-pentadiene	1,3-butadiene	<i>cis</i> -1,3-pentadiene	<i>trans</i> -1,3-pentadiene	1,4-pentadiene
Temperature		±10 K				0.3%		
Impurity (%)	±1%	±11%	±5%	±1%	0.2%	8%	5%	0.2%
Fuel		±5%				1%		
Fitting		5%				5%		
LIF signal		1%				0.2%		
Other (pressure, impurities)						3%		
Root mean square error					7%	11%	8%	7%

1
2
3 At low temperatures, it is generally accepted that olefins + OH reactions undergo almost
4 exclusively via addition channel(s). With some exceptions, e.g., OH reactions with α -terpinene
5 and α -phelandrene, hydrogen abstraction reactions contribute negligibly small (< 10%) to the total
6 rate coefficients of OH + olefins, i.e., $k_{\text{overall}}(T) = k_{\text{addition}}(T) + k_{\text{abstraction}}(T) \approx k_{\text{addition}}(T)$.²³ This
7 means one can simply estimate the overall rate coefficients by summing up the individual rate
8 constants of OH addition to the specific double bond. The more sites an olefin can offer to
9 incoming OH radicals for addition, the more reactive the olefin is. More importantly, their
10 reactivity depends on the type of adduct radical being formed, i.e., primary, secondary, tertiary, or
11 resonantly stabilized.²³ The extent of the stability of the adduct radical will determine the
12 properties of the inner transition states in the potential energy surface of these (poly)olefins + OH
13 reactions and, consequently, the reactivity of these (poly)olefins at low temperatures. In the current
14 case, OH addition to one of the outer carbon atoms of 1,3-pentadiene results into the formation of
15 resonantly stabilized adducts ($\text{OHCH}_2\text{C}\cdot\text{HCH}=\text{CHCH}_3$ or $\text{CH}_2=\text{CHC}\cdot\text{HCH}(\text{OH})\text{CH}_3$). Such
16 resonantly stabilized adduct is not possible for OH addition in 1-pentene, and it offers only two
17 carbon sites for OH addition. Although 1,3-pentadiene has four carbon sites for OH addition, OH
18 preferentially goes to one of the outer carbon atoms to achieve resonance stabilization. This would
19 explain why 1,3-pentadiene shows higher reactivity (~ 4 times) with OH radicals than 1-pentene.
20
21 At low temperatures, in contrary to high temperatures, *cis*- and *trans*- 1,3-pentadienes clearly
22 showed an effect of steric hinderance by displaying differences in the reactivity (see Fig. 2). At
23 298 K, *cis*-conformer of 1,3 pentadiene exhibits ~20% reduction in the reactivity towards OH
24 radicals which is not surprising considering that the OH radicals approaching from the syn side of
25 1,3-pentadiene skeleton gets partly hindered, and thus affecting the formation of the pre-reactive
26 π -complex. At room temperature, we determined a rate coefficient of k_2 (~ 53 mbar) = 1.29×10^{-10}
27 $\text{cm}^3 \text{s}^{-1}$ for *cis*-1,3-pentadiene + OH reaction which matches very well with the values reported by
28 Magneron et al.²⁰ k_2 (1 bar) = $1.21 \times 10^{-10} \text{ cm}^3 \text{ s}^{-1}$) and Ohta et al.¹⁸ k_2 (30 mbar) = $1.02 \times 10^{-10} \text{ cm}^3$
29
30
31
32
33
34
35
36
37
38
39
40
41
42
43
44
45
46
47
48
49
50
51
52
53
54
55
56
57
58
59
60

1
2
3 s⁻¹. This suggests that the measured rate coefficients (k_2) are close to the high-pressure limit.
4
5 Similarly, our value of k_3 (~53 mbar, 294 K) = 1.47×10^{-10} cm³ s⁻¹ for *trans*-1,3-pentadiene + OH
6
7 is in very good agreement with that of Magneron et al.²⁰ k_3 (1 bar, 298 K) = 1.30×10^{-10} cm³ s⁻¹,
8
9 revealing that our low-temperature measurements are also near the high-pressure limit for this
10
11 isomer.
12
13

14
15 As seen in Fig. 2, our low-temperature measurements of 1,3-butadiene + OH reaction at ~ 53 mbar
16
17 compare excellently with the values reported by Grosjean and Williams²¹ ($p \sim 1.3$ mbar) and
18
19 Atkinson et al.²² ($p \sim 67$ mbar). Similar to 1,3-pentadiene + OH reaction, the reaction of 1,3-
20
21 butadiene with OH radicals is close to the high-pressure limit even at a pressure as low as 1 mbar.
22
23 1,3-Butadiene + OH reaction exhibits slower reactivity, roughly by a factor of 2, as compared to
24
25 both conformers of 1,3-pentadienes though these are conjugated dienes and the ensuing adduct
26
27 radicals, after OH addition, are expected to give similar resonance stabilization due to the
28
29 delocalization of the product radicals over three carbon atoms of the conjugated dienes. The
30
31 enhanced reactivity of 1,3-pentadienes may be stemming from the additional contribution of allylic
32
33 hydrogen abstraction which are absent in 1,3-butadiene. The abstraction of allylic hydrogens from
34
35 1,3-pentadiene results in the formation of product radical ($\text{CH}_2=\text{CH}-\text{CH}=\text{CH}-\text{CH}_2^\bullet$) that is super-
36
37 resonantly stabilized. Such super-resonantly stabilized radicals (conjugated allyl) have a resonance
38
39 energy of 19 kcal/mol, roughly 4.78 kcal/mol higher than non-conjugated allyl radical.¹¹ This extra
40
41 stabilization in the product allyl radical enhances the hydrogen abstraction reactions of dienes with
42
43 OH radicals, as seen previously for the reactions of OH radicals with α -terpinene and α -
44
45 phelandrene.⁴⁷ The importance of abstraction reactions of conjugated diolefins to form super-
46
47 resonance stabilized allylic radicals and their major share to the overall rate coefficients at room
48
49 temperature have been reported in the literature.^{23, 47}
50
51
52
53
54
55
56
57
58
59
60

1
2
3 In contrast to the high-temperature chemistry, we observed that at lower temperatures 1,4-
4 pentadiene shows the slowest reactivity towards OH radicals among diolefins. Unlike 1,3-
5 butadiene and 1,3-pentadiene, OH addition to the double bond of 1,4 pentadiene results in an
6 adduct radical that lacks resonance stabilization. This lack of resonance stabilization of the product
7 radical affects the reaction exothercity and the barrier height of the inner transition states forming
8 the adduct radical which ultimately influence the overall reactivity of 1,4-pentadiene with OH
9 radicals. Unlike the case of addition reaction, the ensuing free radical after hydrogen abstraction
10 at the bis-allylic site of 1,4-pentadiene by OH radicals is super-resonantly stabilized due to
11 spreading of unpaired electron out to all five carbon atoms. A recent study has shown that the
12 reaction kinetics of olefins + OH is greatly influenced by both the inner and outer transition states
13 at low temperatures.⁵⁰ Therefore, for 1,4-pentadiene + OH reaction, addition complex does not
14 seem to be as favored as that of 1,3-butadiene and 1,3-pentadiene + OH reactions. Instead, a
15 significant reaction flux may proceed *via* abstraction of secondary allyl hydrogens which leads to
16 the formation of super-resonantly stabilized secondary allyl radicals.

17
18
19
20
21
22
23
24
25
26
27
28
29
30
31
32
33
34
35
36
37
38 Our measured value for k_4 (~ 53 mbar, 294 K) = 5.92×10^{-11} cm³ s⁻¹ compares very well with that
39 from Ohta et al.¹⁸, k_4 (~ 1 bar, 298 K) = 5.06×10^{-11} cm³ s⁻¹, and Atkinson et al.⁵¹, k_4 (~ 1 bar, 298
40 K) = 5.30×10^{-11} cm³ s⁻¹. Similar to the other dienes + OH reactions studied here, the reaction of
41 1,4-pentadiene with OH radicals displays negligible pressure dependence, indicating that the
42 measured values of the rate coefficients are close to the high-pressure limit. Unlike conjugated
43 diolefins + OH reactions where SAR predictions deliver excellent agreement (within 7% of the
44 experimental values),²³ we observe SAR to be not performing as well for 1,4-pentadiene + OH
45 reaction, where the deviation is as large as 30%. Deviations of similar magnitude were also
46 observed for the reactions of OH radicals with other diolefins, e.g., 1,4-hexadiene, α -
47 phenllandrene and α -terpinene. For these olefinic compounds, abstraction reactions are important
48
49
50
51
52
53
54
55
56
57
58
59
60

1
2
3 and their contribution can be significant even at low temperatures. Therefore, SAR prediction by
4 summation of site-specific rate coefficients for OH addition is not adequate for calculating the
5 overall rate coefficients.
6
7
8
9

10
11 Under finite temperatures and pressures of our LPFR/LIF experiments, we did not observe any
12 sign of back dissociation of the addition complex as the loss of OH radicals was purely mono-
13 exponential in all cases. This may have two implications. (i) Conjugated olefins form more stable
14 addition complexes with OH radicals as compared to the non-conjugated olefins, implying quasi-
15 irreversible reaction for the conjugated olefins. In fact, resonantly-stabilized addition complex of
16 1,3-butadiene + OH lands into a well which is ~ 10 kcal/mol deeper as opposed to the non-
17 resonance complex such as propene + OH.¹³ (ii) It may also imply that the inner transition states
18 for the non-abstraction bimolecular channels, which are accessible under our experimental
19 conditions, are submerged below the entrance channel. In either case, the net reaction may well be
20 correlated with the capture rate coefficients. Like (mono)olefins + OH reactions, low-temperature
21 chemistry of diolefins + OH reactions is governed predominantly by addition reactions that
22 typically display negative temperature dependence (see Fig. 2); however, the severity depends on
23 the properties of the outer and inner transition states of these dienes + OH reactions.
24
25
26
27
28
29
30
31
32
33
34
35
36
37
38
39
40
41
42
43
44

45 **4. Summary and Conclusions**

46
47 Rate coefficients for the reaction of hydroxyl radicals with 1,3-butadiene (R1), *cis*- and *trans*-1.3-
48 pentadiene (R2 and R3) and 1,4-pentadiene (R4) were measured over wide range of conditions
49 using two experimental facilities. The measured rate coefficients may be expressed by the
50 following modified Arrhenius expressions (units of $\text{cm}^3\text{molecule}^{-1}\text{s}^{-1}$):
51
52
53
54
55

- 56
57 1. OH + *trans*-1,3-butadiene \rightarrow products (R1) ($T = 881 - 1348$ K, $p \sim 1 - 2.5$ bar and
58 $291 - 468$ K, $p \sim 53$ mbar).
59
60

$$k_1(T) = 3.65 \times 10^4 T^{-5.16} \exp\left(-\frac{1310.8}{T}\right) + 2.49 \times 10^{-18} T^{2.33} \exp\left(-\frac{1850.3}{T}\right) \quad (1)$$

2. OH + *cis*-1,3-pentadiene → products (R2) ($T = 881 - 1348$ K, $p \sim 1 - 2.5$ bar and $291 - 468$ K, $p \sim 53$ mbar).

$$k_2(T) = 5.43 \times 10^4 T^{-5.16} \exp\left(-\frac{1295.8}{T}\right) + 3.18 \times 10^{-17} T^2 \exp\left(-\frac{896.6}{T}\right) \quad (2)$$

3. OH + *trans*-1,3-pentadiene → products (R3) ($T = 881 - 1348$ K, $p \sim 1 - 2.5$ bar and $291 - 468$ K, $p \sim 53$ mbar).

$$k_3(T) = 4.78 \times 10^4 T^{-5.16} \exp\left(-\frac{1204.3}{T}\right) + 3.18 \times 10^{-17} T^2 \exp\left(-\frac{896.6}{T}\right) \quad (3)$$

4. OH + 1,4-pentadiene → products (R4) ($T = 881 - 1348$ K, $p \sim 1 - 2.5$ bar and $291 - 468$ K, $p \sim 53$ mbar).

$$k_4(T) = 2.65 \times 10^{-14} T^{0.86} \exp\left(\frac{808.3}{T}\right) + 1.07 \times 10^{-19} T^{2.93} \exp\left(-\frac{3194.3}{T}\right) \quad (4)$$

Key findings from this work are summarized below :

- Diolefins + OH reactions display complex nature of temperature dependence due to various competing channels. Abstraction channels prevail at high temperatures, while these reactions almost exclusively proceed *via* addition channels at low temperatures; some exceptions are encountered for 1,4-pentadiene + OH reaction.
- At low temperatures ($T < 450$ K), we observed that *trans*-1,3-pentadiene reacts faster than *cis*-1,3-pentadiene due to steric hinderance which impedes the incoming OH radicals to add to *cis*-1,3-pentadiene as opposed to *trans*-1,3-pentadiene. The steric effects are apparent for the differneces in the reactivity of stereo isomers.
- Conjugation in diolefins enhances reactivity towards OH radicals as compared to (mono)olefins at low temperatures, e.g., 1,3-*cis* or *trans*-pentadienes reacts four times faster than 1-pentene with OH radicals.
- Super-resonance stabilization of the allylic adduct radical was found to have a great effect on the reactivity of diolefins + OH reactions at low temperatures. Due to the super allyl resonance, 1,3-pentadiene + OH was found to react faster than 1,3-butadiene + OH, with additional contribution coming from the abstraction of allylic hydrogen atoms.

- 1
2
3
4
5
6
7
8
9
10
11
12
13
14
15
16
17
18
19
20
21
22
23
24
25
26
27
28
29
30
31
32
33
34
35
36
37
- At high temperatures, *cis* and *trans* isomers of 1,3-pentadiene were found to react at similar rates with OH radicals.
 - Diolefins + OH reactions primarily undergo abstraction channels at high temperatures, and the reactivity trends of diolefins + OH reactions depend on the number and type of hydrogen atoms being abstracted, e.g., primary, secondary, tertiary, vinylic, allylic or super-allylic. Hydrogen abstraction from the allylic site of 1,3-pentadienes and 1,4-pentadiene becomes the major active channel at high temperatures, explaining the higher reactivity of these dienes with OH radicals than that of 1,3-butadiene.
 - Addition and non-abstraction channels can make a significant share to the total rate coefficients even at 1000 K due to the resonance stabilization of the adduct radicals of conjugated diene + OH reactions.
 - For the 1,4,-pentadiene + OH reaction, addition complex does not seem to be as favored as that of 1,3-butadiene and 1,3-pentadiene + OH reactions. Instead, a significant reaction flux may proceed *via* abstraction even at low temperatures.

38 **Acknowledgements**

39
40
41
42
43
44
45
46
47
48
49
50
51
52
53
54
55
56
57
58
59
60

Research reported in this work was funded by King Abdullah University of Science and Technology (KAUST). Work in Lille was funded by by the French ANR agency under contract No. ANR-11-LabX-0005-01 CaPPA (Chemical and Physical Properties of the Atmosphere) and the Région Hauts-de-France, the Ministère de l'Enseignement Supérieur et de la Recherche and the European Fund for Regional Economic Development (CPER Climibio).

References

1. OECD, *Oil 2018: Analysis and Forecasts to 2023*. 2018; p 137.
2. Kalghatgi, G. T., The outlook for fuels for internal combustion engines. *Int. J. Engine Res.* **2014**, *15* (4), 383-398.
3. Kalghatgi, G. T., Developments in internal combustion engines and implications for combustion science and future transport fuels. *Proc. Combust.Inst* **2015**, *35* (1), 101-115.
4. Kalghatgi, G. T., *Fuel/engine interactions*. SAE International Warrendale, PA: 2014.
5. Sarathy, S. M.; Kukkadapu, G.; Mehl, M.; Javed, T.; Ahmed, A.; Naser, N.; Tekawade, A.; Kosiba, G.; AlAbbad, M.; Singh, E.; Park, S.; Rashidi, M. A.; Chung, S. H.; Roberts, W. L.; Oehlschlaeger, M. A.; Sung, C.-J.; Farooq, A., Compositional effects on the ignition of FACE gasolines. *Combust. Flame* **2016**, *169*, 171-193.
6. Sarathy, S. M.; Kukkadapu, G.; Mehl, M.; Wang, W.; Javed, T.; Park, S.; Oehlschlaeger, M. A.; Farooq, A.; Pitz, W. J.; Sung, C.-J., Ignition of alkane-rich FACE gasoline fuels and their surrogate mixtures. *Proc. Combust.Inst* **2015**, *35* (1), 249-257.
7. Energy, U. S. D. o. *Co-Optimization of Fuels and Engines*; 2016.
8. Westbrook, C. K.; Mehl, M.; Pitz, W. J.; Sjöberg, M., Chemical kinetics of octane sensitivity in a spark-ignition engine. *Combust. Flame* **2017**, *175*, 2-15.
9. Leppard, W. R., The Chemical Origin of Fuel Octane Sensitivity. SAE International: 1990.
10. Westbrook, C. K.; Pitz, W. J.; Mehl, M.; Glaude, P.-A.; Herbinet, O.; Bax, S.; Battin-Leclerc, F.; Mathieu, O.; Petersen, E. L.; Bugler, J.; Curran, H. J., Experimental and Kinetic Modeling Study of 2-Methyl-2-Butene: Allylic Hydrocarbon Kinetics. *J. Phys. Chem. A* **2015**, *119* (28), 7462-7480.
11. Senosiain, J. P.; Han, J. H.; Musgrave, C. B.; Golden, D. M., Use of quantum methods for a consistent approach to combustion modelling: Hydrocarbon bond dissociation energies. *Faraday Discuss.* **2002**, *119* (0), 173-189.
12. Puhan, S.; Saravanan, N.; Nagarajan, G.; Vedaraman, N., Effect of biodiesel unsaturated fatty acid on combustion characteristics of a DI compression ignition engine. *Biomass Bioenergy* **2010**, *34* (8), 1079-1088.
13. Vasu, S. S.; Zádor, J.; Davidson, D. F.; Hanson, R. K.; Golden, D. M.; Miller, J. A., High-Temperature Measurements and a Theoretical Study of the Reaction of OH with 1, 3-butadiene. *J. Phys. Chem. A* **2010**, *114* (32), 8312-8318.
14. Vasu, S. S.; Huynh, L. K.; Davidson, D. F.; Hanson, R. K.; Golden, D. M., Reactions of OH with Butene Isomers: Measurements of the Overall Rates and a Theoretical Study. *J. Phys. Chem. A* **2011**, *115* (12), 2549-2556.
15. Khaled, F.; Badra, J.; Farooq, A., A shock tube study of C4–C6 straight chain alkenes+OH reactions. *Proc. Combust.Inst* **2017**, *36* (1), 289-298.
16. Granata, S.; Faravelli, T.; Ranzi, E.; Olten, N.; Senkan, S., Kinetic modeling of counterflow diffusion flames of butadiene. *Combust. Flame* **2002**, *131* (3), 273-284.
17. Goldaniga, A.; Faravelli, T.; Ranzi, E., The kinetic modeling of soot precursors in a butadiene flame. *Combust. Flame* **2000**, *122* (3), 350-358.
18. Ohta, T., Rate constants for reactions of diolefins with hydroxyl radicals in the gas phase. Estimate of the rate constants from those for monoolefins. *J. Phys. Chem.* **1983**, *87* (7), 1209-1213.
19. McGillen, M. R.; Percival, C. J.; Shallcross, D. E.; Harvey, J. N., Is hydrogen abstraction an important pathway in the reaction of alkenes with the OH radical? *Phys. Chem. Chem. Phys.* **2007**, *9* (31), 4349-4356.
20. Magneron, I.; Mellouki, A.; Le Bras, G.; Moortgat, G.; Horowitz, A.; Wirtz, K., Photolysis and OH-initiated oxidation of glycolaldehyde under atmospheric conditions. *J. Phys. Chem. A* **2005**, *109* (20), 4552-4561.

- 1
2
3 21. Grosjean, D.; Williams Ii, E. L., Environmental persistence of organic compounds
4 estimated from structure-reactivity and linear free-energy relationships. Unsaturated aliphatics.
5 *Atmos. Environ., Part A* **1992**, *26* (8), 1395-1405.
- 6 22. Atkinson, R.; Perry, R.; Pitts Jr, J., Absolute rate constants for the reaction of OH radicals
7 with allene, 1, 3-butadiene, and 3-methyl-1-butene over the temperature range 299–424° K. *J.*
8 *Chem. Phys.* **1977**, *67* (7), 3170-3174.
- 9 23. Peeters, J.; Boullart, W.; Pultau, V.; Vandenberg, S.; Vereecken, L., Structure–Activity
10 Relationship for the Addition of OH to (Poly)alkenes: Site-Specific and Total Rate Constants. *J.*
11 *Phys. Chem. A* **2007**, *111* (9), 1618-1631.
- 12 24. D. King, M.; E. Canosa-Mas, C.; P. Wayne, R., A structure-activity relationship (SAR)
13 for predicting rate constants for the reaction of NO₃, OH and O₃ with monoalkenes and conjugated
14 dienes. *Phys. Chem. Chem. Phys.* **1999**, *1* (9), 2239-2246.
- 15 25. Atkinson, R.; Arey, J., Atmospheric Degradation of Volatile Organic Compounds. *Chem.*
16 *Rev.* **2003**, *103* (12), 4605-4638.
- 17 26. Li, Y.; O'Connor, E.; Zhou, C.-W.; Curran, H. J. In *An experimental study of butene*
18 *isomers and 1, 3-butadiene ignition delay times at elevated pressures*, European Combustion
19 Meeting, 2015.
- 20 27. Li, Y.; Klippenstein, S. J.; Zhou, C.-W.; Curran, H. J., Theoretical Kinetics Analysis for
21 H Atom Addition to 1,3-Butadiene and Related Reactions on the C₄H₇ Potential Energy Surface.
22 *J. Phys. Chem. A* **2017**, *121* (40), 7433-7445.
- 23 28. Li, Z.; Nguyen, P.; Fatima de Leon, M.; Wang, J. H.; Han, K.; He, G. Z., Experimental
24 and Theoretical Study of Reaction of OH with 1,3-Butadiene. *J. Phys. Chem. A* **2006**, *110* (8),
25 2698-2708.
- 26 29. Guenther, A.; Hewitt, C. N.; Erickson, D.; Fall, R.; Geron, C.; Graedel, T.; Harley, P.;
27 Klinger, L.; Lerdau, M.; McKay, W., A global model of natural volatile organic compound
28 emissions. *J. Geophys. Res.: Atmos.* **1995**, *100* (D5), 8873-8892.
- 29 30. Guenther, A.; Geron, C.; Pierce, T.; Lamb, B.; Harley, P.; Fall, R., Natural emissions of
30 non-methane volatile organic compounds, carbon monoxide, and oxides of nitrogen from North
31 America. *Atmos. Environ.* **2000**, *34* (12), 2205-2230.
- 32 31. Sawyer, R. F.; Harley, R. A.; Cadle, S. H.; Norbeck, J. M.; Slott, R.; Bravo, H. A.,
33 Mobile sources critical review: 1998 NARSTO assessment. *Atmos. Environ.* **2000**, *34* (12), 2161-
34 2181.
- 35 32. Atkinson, R., A structure-activity relationship for the estimation of rate constants for the
36 gas-phase reactions of OH radicals with organic compounds. *Int. J. Chem. Kinet.* **1987**, *19* (9),
37 799-828.
- 38 33. Kwok, E. S. C.; Atkinson, R., Estimation of hydroxyl radical reaction rate constants for
39 gas-phase organic compounds using a structure-reactivity relationship: An update. *Atmos.*
40 *Environ.* **1995**, *29* (14), 1685-1695.
- 41 34. Pfrang, C.; King, M. D.; Canosa-Mas, C. E.; Wayne, R. P., Structure–activity relations
42 (SARs) for gas-phase reactions of NO₃, OH and O₃ with alkenes: An update. *Atmos. Environ.*
43 **2006**, *40* (6), 1180-1186.
- 44 35. Badra, J.; Elwardany, A. E.; Khaled, F.; Vasu, S. S.; Farooq, A., A shock tube and laser
45 absorption study of ignition delay times and OH reaction rates of ketones: 2-Butanone and 3-buten-
46 2-one. *Combust. Flame* **2014**, *161* (3), 725-734.
- 47 36. Badra, J.; Khaled, F.; Giri, B. R.; Farooq, A., A shock tube study of the branching ratios
48 of propene+ OH reaction. *Physical Chemistry Chemical Physics* **2015**, *17* (4), 2421-2431.
- 49 37. Campbell, M. F.; Haylett, D. R.; Davidson, D. F.; Hanson, R. K., AEROFROSH: a shock
50 condition calculator for multi-component fuel aerosol-laden flows. *Shock Waves* **2015**, 1-19.
- 51 38. Bradley, J., Shock waves in physics and chemistry. *Methuen, London* **1962**.
- 52
53
54
55
56
57
58
59
60

- 1
2
3 39. Benson, S. W.; O'Neal, H. E. *Kinetic data on gas phase unimolecular reactions*; DTIC
4 Document: 1970.
- 5 40. Parker, A.; Jain, C.; Schoemaeker, C.; Fittschen, C., Kinetics of the reaction of OH
6 radicals with CH₃OH and CD₃OD studied by laser photolysis coupled to high repetition rate laser
7 induced fluorescence. *React. Kinet. Catal. Lett.* **2009**, *96* (2), 291-297.
- 8 41. Assaf, E.; Fittschen, C., Cross Section of OH Radical Overtone Transition near 7028 cm⁻¹
9 and Measurement of the Rate Constant of the Reaction of OH with HO₂ Radicals. *J. Phys. Chem.*
10 *A* **2016**, *120* (36), 7051-7059.
- 11 42. Assaf, E.; Song, B.; Tomas, A.; Schoemaeker, C.; Fittschen, C., Rate Constant of the
12 Reaction between CH₃O₂ Radicals and OH Radicals revisited. *J. Phys. Chem. A* **2016**, *120* (45),
13 8923-8932.
- 14 43. Pang, G. A.; Hanson, R. K.; Golden, D. M.; Bowman, C. T., High-Temperature
15 Measurements of the Rate Constants for Reactions of OH with a Series of Large Normal Alkanes:
16 n-Pentane, n-Heptane, and n-Nonane. *Z. Phys. Chem.* **2011**, *225* (11-12), 1157-1178.
- 17 44. Mehl, M.; Pitz, W. J.; Westbrook, C. K.; Curran, H. J., Kinetic modeling of gasoline
18 surrogate components and mixtures under engine conditions. *Proc. Combust. Inst.* **2011**, *33* (1),
19 193-200.
- 20 45. Giri, B. R.; Szori, M.; Liu, D.; Khalid, F.; Mai, T. V.-T.; Huynh, L. K.; Viskolcz, B.;
21 Farooq, A., An Experimental and Theoretical Kinetic Study of the Reaction of Hydroxyl Radicals
22 with 1,4-Pentadiene. *Journal of Chemical Theory and Computation*
23 **2018**.
- 24 46. Marley, W. M.; Jeffers, P. M., Shock tube cis-trans isomerization studies. IV. *J. Phys.*
25 *Chem.* **1975**, *79* (20), 2085-2087.
- 26 47. Vereecken, L.; Peeters, J., H-atom abstraction by OH-radicals from (biogenic)
27 (poly)alkenes: C-H bond strengths and abstraction rates. *Chem. Phys. Lett.* **2001**, *333* (1-2), 162-
28 168.
- 29 48. Zádor, J.; Jasper, A. W.; Miller, J. A., The reaction between propene and hydroxyl. *Phys.*
30 *Chem. Chem. Phys.* **2009**, *11* (46), 11040-11053.
- 31 49. Zador, J.; Jasper, A. W.; Miller, J. A., The reaction between propene and hydroxyl. *Phys*
32 *Chem Chem Phys* **2009**, *11* (46), 11040-53.
- 33 50. Greenwald, E. E.; North, S. W.; Georgievskii, Y.; Klippenstein, S. J., A two transition
34 state model for radical-molecule reactions: applications to isomeric branching in the OH-isoprene
35 reaction. *J. Phys. Chem. A* **2007**, *111* (25), 5582-92.
- 36 51. Atkinson, R., Gas-Phase Tropospheric Chemistry of Volatile Organic Compounds: 1.
37 Alkanes and Alkenes. *Journal of Physical and Chemical Reference Data* **1997**, *26* (2), 215-290.
38
39
40
41
42
43
44
45
46
47
48
49
50
51
52
53
54
55
56
57
58
59
60